

Synthesis and Characterization of a New Compound with Alternating MnO_2^{2-} and $\text{Zn}_2\text{As}_2^{2-}$ Layers: $\text{Ba}_2\text{MnZn}_2\text{As}_2\text{O}_2$

Tadashi Ozawa, Marilyn M. Olmstead, Stephanie L. Brock,[†] and Susan M. Kauzlarich*

Department of Chemistry, One Shields Avenue, University of California, Davis, California 95616

Dianna M. Young

Intense Pulsed Neutron Source, Argonne National Laboratory, Argonne, Illinois 60439

Received August 8, 1997. Revised Manuscript Received November 12, 1997

A new mixed transition metal pnictide oxide, $\text{Ba}_2\text{MnZn}_2\text{As}_2\text{O}_2$, is reported. $\text{Ba}_2\text{MnZn}_2\text{As}_2\text{O}_2$ has been prepared in quantitative yield from heating stoichiometric amounts of BaO with the elements, which are pressed into a pellet, placed in an Al_2O_3 boat, and sealed in a fused silica ampule, at 1000 °C. This compound is an ordered variant of the $\text{Sr}_2\text{Mn}_3\text{As}_2\text{O}_2$ structure type and crystallizes in the tetragonal space group $I4/mmm$ ($Z = 2$). Single-crystal X-ray data (130 K) were refined ($a = 4.2317(3)$ Å, $c = 19.443(2)$ Å, $R1 = 2.96\%$, $wR2 = 6.84\%$). The structure is made up from square planar MnO_2 layers with layers of Zn_2As_2 tetrahedra interspersed by alkaline earth cations such that the formula may be written as $\text{Ba}_2(\text{MnO}_2)(\text{Zn}_2\text{As}_2)$. Rietveld refinement ($a = 4.24257(8)$ Å, $c = 19.5087(7)$ Å, $R_{\text{wp}} = 9.26\%$, $R_p = 6.44\%$) of powder neutron diffraction data obtained at room temperature provides unambiguous evidence for this ordered model in the case of $\text{Ba}_2\text{MnZn}_2\text{As}_2\text{O}_2$. Magnetic studies in the temperature range $5 \leq T/K \leq 300$ show antiferromagnetic ordering at 38 K with spin glasslike behavior at low temperatures.

Introduction

This group has explored the magnetic and electronic properties of a small class of layered compounds referred to as pnictide oxides.^{1–6} These compounds are unusual in that both the pnictogen and the oxygen are present as anions rather than being covalently bound as a pnictate ion (PnO_4^{3-}). Several structure types exist in this class, of which the $\text{Sr}_2\text{Mn}_3\text{As}_2\text{O}_2$ -type⁷ has been the most studied. This structure type shows an interesting segregation of layers where the square-planar metal oxide layers are sandwiched by tetrahedrally coordinated metal pnictide layers with alkaline earth cations interspersed between the layers. In addition to the pnictide oxides, there is also an example of a mixed layered phase in the chalcogenide oxide system which could be described as a variant of this structure type.⁸ Recently, the compounds $\text{Sr}_2\text{Cu}_2\text{MO}_2\text{S}_2$ ($M = \text{Mn, Co,}$

Zn) have been prepared and characterized.⁹ These compounds are isostructural with $\text{Sr}_2\text{Mn}_3\text{As}_2\text{O}_2$ ⁷ with $\text{Cu}_2\text{S}_2^{2-}$ layers and MO_2^{2-} layers. Copper is present as Cu^{I} , and the M is present as M^{II} . There has been recent interest in layered pnictide oxides, and a number of new compounds have been prepared with an aim toward finding a cuprate analogue,¹⁰ which one might expect to be superconducting because of the square-planar oxide site. Another aim of this research is to prepare materials with unusual magnetic and electronic properties, and several rare earth Fe, Co, Ni, and Cu pnictide oxides have been recently prepared.^{11,12} Compounds of the general formula $\text{A}_2\text{M}_3\text{Pn}_2\text{O}_2$ ($A =$ alkaline earth, $M =$ transition metal, $\text{Pn} =$ pnictogen), are known for the alkaline earth elements Ba and Sr and for the transition metal Mn and crystallize in the $\text{Sr}_2\text{Mn}_3\text{As}_2\text{O}_2$ structure type ($I4/mmm$).^{1,7} This structure type has two different layers, one composed of $\text{Mn}_2\text{As}_2^{2-}$ units and the other composed of MnO_2^{2-} units. The layers alternated within the structure along the c axis. The bonding within the layers is covalent and the layers are held together via ionic bonding to the interpenetrating

* To whom correspondence should be addressed.

[†] Current address: Department of Chemistry, University of Connecticut, 215 Glenbrook Rd., U-60, Storrs, CT 06269.

(1) Stetson, N. T.; Kauzlarich, S. M. *Inorg. Chem.* **1991**, *30*, 3969.

(2) Brock, S. L.; Hope, H.; Kauzlarich, S. M. *Inorg. Chem.* **1994**, *33*, 405.

(3) Brock, S. L.; Kauzlarich, S. M. *Inorg. Chem.* **1994**, *33*, 2491.

(4) Brock, S. L.; Kauzlarich, S. M. *Comments Inorg. Chem.* **1995**, *17*, 213.

(5) Brock, S. L.; Kauzlarich, S. M. *Chem. Tech.* **1995**, *25*, 18.

(6) Brock, S. L.; Raju, N. P.; Greedan, J. E.; Kauzlarich, S. M. *J. Alloys Compd.* **1996**, *237*, 9.

(7) Brechtel, E.; Cordier, G.; Schäfer, H. *Z. Naturforsch. B* **1979**, *34*, 777.

(8) Park, Y.; DeGroot, D. C.; Schindler, J. L.; Kannewurf, C. R.; Kanatzidis, M. G. *Chem. Mater.* **1993**, *5*, 8.

(9) Zhu, W. J.; Hor, P. H. *J. Sol. State Chem.* **1997**, *130*, 319 and references therein.

(10) Cava, R. J.; Zanbergen, H. W.; Krajewski, J. J.; Siegrist, T.; Hwang, H. Y.; Batlogg, B. *J. Solid State Chem.* **1997**, *129*, 250.

(11) Albering, J. H.; Jeitschko, W. *Z. Naturforsch.* **1996**, *51b*, 257.

(12) Zimmer, B. I.; Jeitschko, W.; Albering, J. H.; Glaum, R.; Reehuis, M. *J. Alloys Compd.* **1995**, *229*, 238.

alkaline earth cations. The Mn compounds show antiferromagnetic coupling.¹³ Neutron diffraction studies of $\text{Sr}_2\text{Mn}_3\text{Sb}_2\text{O}_2$ and $\text{Sr}_2\text{Mn}_3\text{As}_2\text{O}_2$ have been performed and show that this layered structure has two independent magnetic lattices.^{6,13} We have recently prepared Zn compounds of the $\text{Sr}_2\text{Mn}_3\text{As}_2\text{O}_2$ structure type in which Zn replaces the Mn atoms.³ These compounds are unique in that a square-planar environment is unusual for Zn, especially in an extended solid. The Zn compounds are diamagnetic semiconductors. The idea of exploring the continuum between the diamagnetic Zn phase and antiferromagnetic Mn phase is intriguing. One might expect to find new properties and in addition provide insight into the magnetic interactions in this layer phase. Since the Mn and the Zn compounds are isostructural, we decided to explore the solid solution compounds corresponding to $\text{Ba}_2\text{Mn}_{3-x}\text{Zn}_x\text{As}_2\text{O}_2$. This paper presents the synthesis and characterization of the ordered compound $\text{Ba}_2\text{MnZn}_2\text{As}_2\text{O}_2$ in which Mn resides in the MO_2^{2-} layers and Zn resides in the $\text{M}_2\text{As}_2^{2-}$ layers. This is the first example of a mixed metal pnictide phase with site preference in this structure type. Powder neutron diffraction and single-crystal X-ray diffraction data are consistent with the ordered model for $\text{Ba}_2\text{MnZn}_2\text{As}_2\text{O}_2$. $\text{Ba}_2\text{MnZn}_2\text{As}_2\text{O}_2$ has additionally been characterized by powder X-ray diffraction and temperature-dependent magnetic susceptibility.

Experimental Procedures

Synthesis. BaO was prepared from thermal decomposition of BaCO_3 (J. Matthey, 99.99%) under vacuum (1000 °C, 48 h). Mn flake (J. Matthey, 99.98%) was etched with 15 vol % HNO_3 in methanol and rinsed with acetone before pumping into a drybox. The Mn was ground into a powder in the drybox. Zn (Fisher Scientific, 99.4%) and As (J. Matthey, 99.999%) were used as received. The compound $\text{Ba}_2\text{MnZn}_2\text{As}_2\text{O}_2$ was synthesized by heating a pressed pellet of BaO, Mn, Zn, As (2:1:2:2) in an alumina boat sealed in a fused silica ampule under $1/5$ atm of argon at 1000 °C for 1 week. The product was a black microcrystalline powder. Single crystals were prepared by ramping the temperature at a rate of 60 °C/h. The crystals were black and very small with a platelike habit. The yield estimated from powder X-ray diffraction was quantitative, and there were no other phases present. The compound is stable in air for long periods of time. A 5 g sample was prepared for powder neutron diffraction. There is a small amount of unidentified impurity that is present in that sample.

Structural Characterization. Powder neutron diffraction was performed on the general purpose powder diffractometer (GPPD) at the Intense Pulsed Neutron Source. The refinement is from data taken with the detectors with scattering angles $\pm 90^\circ$. Including the data from the $\pm 148^\circ$ detector banks gives similar results. The $\text{Ba}_2\text{MnZn}_2\text{As}_2\text{O}_2$ sample was placed in an airtight vanadium container under a helium atmosphere, and data were collected at room temperature. Rietveld refinements using time-of-flight neutron powder data were carried out using GSAS (general structure analysis system).¹⁴ Lattice parameters and atomic positions were initially obtained from published single-crystal X-ray results of $\text{Ba}_2\text{Zn}_3\text{As}_2\text{O}_2$ ($I4/mmm$).³ A six-coefficient cosine Fourier series model was refined to fit the background. Powder X-ray diffraction data from the sample indicated that small amounts

of impurities were present, but it was not significant for neutron data refinement. The $\text{Ba}_2\text{MnZn}_2\text{As}_2\text{O}_2$ material was of high crystallinity, and no corrections for amorphous material were made. Peak profiles, lattice parameters, atomic positions, absorption, and extinction were also refined. Mn has a negative scattering length (-0.373×10^{-12} cm) and Zn has a positive scattering length (0.568×10^{-12} cm). To establish the degree of chemical preference between Zn and Mn, an initial refinement was made with no chemical distinction between the sites 2a and 4d, i.e., refined $\text{Ba}_2\text{Zn}_3\text{As}_2\text{O}_2$. The refinement made it clear that Mn was located on the 2a site because a negative fraction value was obtained when Zn was refined on the 2a site. The Mn occupancy in site 2a and the Zn occupancy in site 4d were refined to 1.000(1) and 0.999(1), respectively; for subsequent refinement cycles, occupancy was constrained to unity. There was no evidence of mixed metals on these sites. Anisotropic refinement of temperature factors was also performed.

Single-crystal X-ray diffraction was performed at low temperature (130 K) with a Siemens P4 diffractometer equipped with a LT-2 low-temperature apparatus. A black plate of dimensions $0.004 \times 0.024 \times 0.080$ mm was selected from a batch with prevalent twinning that contained no larger specimens. It was mounted in the cold stream (130 K) of the diffractometer. The radiation employed was Ni-filtered Cu $K\alpha$ from a Siemens rotating anode source operating at 15 kW. A full sphere of data was collected to a maximum 2θ of 113° . Less than 0.1% fluctuation in the intensities of two standard reflections was observed during the data collection. A lamina model of ψ -scans absorption correction was applied.¹⁵ The structure was solved using direct methods.^{15b} Refinement was by full-matrix least-squares methods, based on F^2 , using all data.^{15c} Several models were investigated, including Mn in both the 2a and 4d site, Zn in both the 2a and 4d site, and a random distribution of Mn and Zn in the 2a and 4d sites. In all cases, the $wR2$ was significantly larger than in the solution with Mn in the 2a site and Zn in the 4d site, indicating that this is the best model. The largest peak in the final difference map was $1.18 \text{ e } \text{\AA}^{-3}$. Additional single-crystal X-ray diffraction and refinement data are provided as Supporting Information.

Powder X-ray diffraction was performed on a Siemens D500 X-ray diffractometer. Data were collected at room temperature using Cu $K\alpha$ radiation. The powder pattern was scanned over $20\text{--}120^\circ$ at 0.02° step for 10 s/step. Rietveld refinement was performed utilizing the GSAS software package.¹⁴ For $\text{Ba}_2\text{MnZn}_2\text{As}_2\text{O}_2$, lattice and positional parameters were taken from the neutron data of the same compound. Lattice parameters, background coefficients (power series in $q^{2n}/n!$ and $n!/q^{2n}$), preferred orientation parameters (spherical harmonic model), atomic position, isotropic thermal factors, and profile coefficients were refined. The neutron model gave a good fit to the X-ray powder diffraction data. Refinement parameters are provided as Supporting Information.

Magnetic Susceptibility Measurements. A Quantum Design SQUID magnetometer was employed for making magnetic measurements. Magnetic data were collected on powder samples sealed in a fused silica tube, designed to provide negligible background, under vacuum. Magnetization vs field data were taken at 5, 12, 60, 64, and 66 K over the range 0–10 000 Oe, and the magnetization data at 12 K and higher temperatures show a linear dependence upon field, consistent with field-independent magnetic susceptibility. The 5 K data show a small deviation from linearity. Magnetization vs temperature data were obtained from 5 to 300 K in a field of 5 kOe. This field was chosen in order to compare these results to those obtained for the all-Mn containing com-

(13) Brock, S. L.; Kauzlarich, S. M. *J. Alloys Compd.* **1996**, *241*, 82.

(14) Larson, A. C.; Von Dreele, R. B. *GSAS, General Structure Analysis System*, LANSCE, MS-H805, Los Alamos National Laboratory, Los Alamos, NM 87545, 1990.

(15) Crystallographic programs were those of SHELXTL v. 5.03. G. Sheldrick, 1994. Distributed by Siemens Industrial Automation, Inc. Madison, WI. Tables of neutral atom scattering factors, f' and f'' , and absorption coefficients are from: *International Tables for Crystallography*, Wilson, A. J. C., Ed.; Kluwer Academic Publishers: Dordrecht, 1992; Vol. C, Tables 6.1.1.3 (pp 500–502), 4.2.6.8 (pp 219–222), and 4.2.4.2 (pp 193–199), respectively. (a) XPREP subroutine; (b) XS; (c) XL.

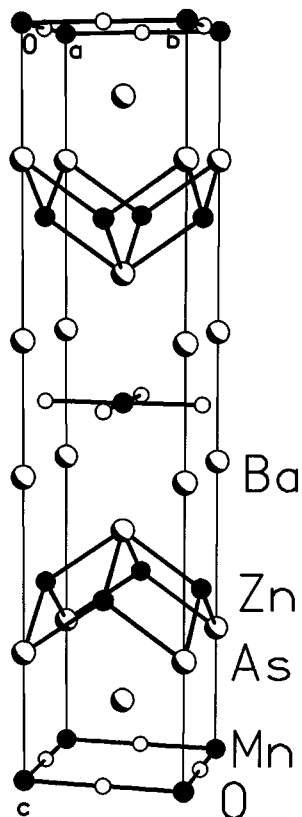


Figure 1. Perspective view of the structure of $\text{Ba}_2\text{MnZn}_2\text{As}_2\text{O}_2$.

pounds.¹³ Temperature-dependent zero-field cooled (ZFC) and field cooled (FC) magnetization data were collected.

Results and Discussion

Figure 1 shows a view of the structure of $\text{Ba}_2\text{MnZn}_2\text{As}_2\text{O}_2$. The structure is composed of alternating layers of $\text{Zn}_2\text{As}_2^{2-}$ and MnO_2^{2-} anionic nets separated by the Ba cations. The Ba cation resides in a square antiprism composed of four As atoms from the $\text{Zn}_2\text{As}_2^{2-}$ layer and four O atoms from the MnO_2^{2-} layer. Since the scattering factor for neutron diffraction of Mn is negative, the assignment of metals to a particular layer is unambiguous. Despite the fact that both end members can be made, the coordination preferences of the different metals are manifested in the solid solution. Figure 2 shows the fit of the model to the neutron powder diffraction data. This result is consistent with the refinement of powder X-ray diffraction (Figure 3) as well as refinement of single-crystal X-ray data in which the best model proves to be the ordered structure with $\text{Zn}_2\text{As}_2^{2-}$ layers and MnO_2^{2-} layers. Lattice parameters for $\text{Ba}_2\text{MnZn}_2\text{As}_2\text{O}_2$ are provided in Table 1 along with refinement data. These parameters are intermediate between the all-Mn ($a = 4.248(5)$, $c = 19.77(3)$ Å)^{7,13} and the all-Zn ($a = 4.0954(7)$, $c = 18.918(4)$ Å)³ phase. Table 2 provides positional parameters and anisotropic displacement parameters obtained from the refinement of the powder neutron diffraction data. The refinement of the structure from the single-crystal and powder X-ray diffraction data provided a model in good agreement with that obtained from the neutron data. Table 3 provides distances from the powder neutron diffraction data refinement. The Zn–As bond distance is 2.5848-

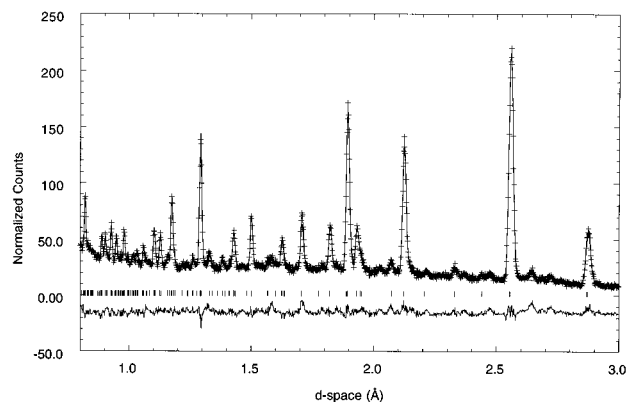


Figure 2. Profile fit and difference plots for the Rietveld refinement of neutron diffraction data for $\text{Ba}_2\text{MnZn}_2\text{As}_2\text{O}_2$. The short vertical markers represent allowed reflections.

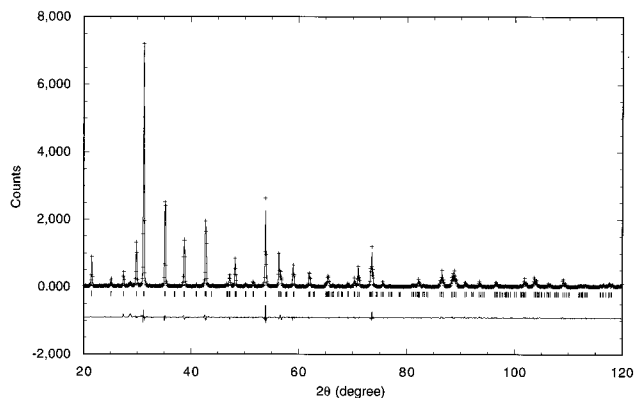


Figure 3. Profile fit and difference plots for the Rietveld refinement of X-ray diffraction data for $\text{Ba}_2\text{MnZn}_2\text{As}_2\text{O}_2$. The short vertical markers represent allowed reflections.

Table 1. Crystallographic Parameters for $\text{Ba}_2\text{MnZn}_2\text{As}_2\text{O}_2$ (Space Group $I4/mmm$)^a

	powder neutron diffraction ^a	powder X-ray diffraction	single-crystal X-ray diffraction
a (Å)	4.24257(8)	4.23369(4)	4.2317(3)
c (Å)	19.5087(7)	19.4780(3)	19.443(2)
Z	2	2	2
ρ_{calc} , g cm ⁻³	6.074	6.109	6.126
R_{wp} (%)	9.26	15.20	
R_{p} (%)	6.44	9.92	
χ^2	2.648	2.211	
$R1$ (%)			2.96
$wR2$ (%)			6.84
no. of parameters	24	33	15
temp (K)	295	295	130(2)

^a $R_{\text{wp}} = [M/\sum(wI_0^2)]^{1/2}$; $R_{\text{p}} = \sum|I_0 - I_c|/\sum I_0$; $R1 = \sum|F_0 - F_c|/\sum|F_0|$; $wR2 = [\sum[w(F_0^2 - F_c^2)^2]/\sum[w(F_0^2)^2]]^{1/2}$.

(12) Å, which is very slightly larger than that observed in the all-Zn compound (2.5785(6) Å),³ but is consistent with the range expected for tetrahedral ZnAs_4 units in other solid-state compounds.^{16,17} The Mn–O distance is 2.1158(1) Å, very slightly smaller than that found in the all-Mn compound (2.124(0) Å).⁷ The flexibility of bond distances within the two layers allows for lattice matching which permits the formation of this mixed metal compound. The Mn is capped by As atoms from the planes above and below. The long Mn⋯As distance of 3.376(1) Å precludes any Mn–As bonding between the two layers.

Figure 4 shows the zero field cooled (ZFC) and field cooled (FC) magnetic susceptibility for the $\text{Ba}_2\text{MnZn}_2\text{As}_2\text{O}_2$.

Table 2. Atomic Coordinates ($\times 10^4$) and Displacement Coefficients ($\text{\AA}^2 \times 10^3$)^a Obtained from the Rietveld Refinement of Powder Neutron Diffraction Data for $\text{Ba}_2\text{MnZn}_2\text{As}_2\text{O}_2$ ^a

atom	site sym	x	y	z	$U(\text{eq})$	U_{11}	U_{33}
Ba	4e	0	0	4099(2)	1.6(1)	0.8(1)	1.1 (1)
Mn	2a	0	0	0	5.9(4)	4.0(3)	7.7(7)
Zn	4d	0	5000	2500	1.8(1)	1.3(1)	0.8(1)
As	4e	0	0	1743(3)	1.0(1)	0.8(1)	0.3(1)
O	4c	0	5000	0	1.7(1)	0.8(1)	1.5(1)

^a $U(\text{eq})$ is defined as one-third of the trace of the orthogonalized U_{ij} tensor. The anisotropic displacement factor exponent takes the form $-2\pi^2[(ha^*)^2 U_{11} + \dots + 2hka^*b^* U_{12}]$. $U_{11} = U_{22}$; $U_{23} = U_{13} = U_{12} = 0$.

Table 3. Interatomic Distances (\AA) in $\text{Ba}_2\text{MnZn}_2\text{As}_2\text{O}_2$ ^a

Ba–O(1)	2.7460(7)
Ba–Mn	3.4666(6)
Zn–Zn	2.9923(2)
Ba–As	3.4053(11)
Mn–O	2.1158(1)
Zn–As	2.5848(12)
Zn–Ba	3.7618(9)

^a Determined from powder neutron diffraction data.

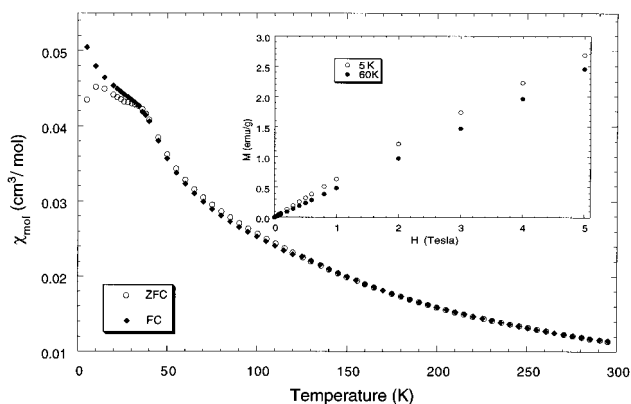


Figure 4. Magnetic susceptibility as a function of temperature of $\text{Ba}_2\text{MnZn}_2\text{As}_2\text{O}_2$ measured at 5 kOe, zero field cooled (ZFC) and field cooled (FC). The inset shows the magnetization versus field data at 5 and 60 K.

As_2O_2 compound along with the field dependence of the magnetization at 5 and 60 K. The inset shows the magnetization data as a function of field. The data taken at 60 K are linear, consistent with field-independent susceptibility, and provides evidence for no ferromagnetic impurities in this sample. The data taken at 5 K show a very small deviation from linearity which is consistent with the low-temperature behavior of the sample. The susceptibility shows a lower temperature ordering at 38 K, unlike the all-Mn containing compound which shows a broad antiferromagnetic transition at 100 K.¹³ At about 30 K there is a small divergence of the ZFC and magnetization which becomes significant at 12 K. This may be interpreted as spin glass behavior with a freezing temperature of 12 K. This is in sharp contrast to the magnetic susceptibility data for $\text{Ba}_2\text{Mn}_3\text{As}_2\text{O}_2$, which has identical data for ZFC and FC magnetization.¹³ The overall susceptibility of $\text{Ba}_2\text{MnZn}_2\text{As}_2\text{O}_2$ is approximately 5 times larger than for the all-Mn containing compound. Fitting the data above 180 K to the Curie–Weiss law gives $\theta = -51(5)$ K and an effective moment of $5.7(1) \mu_B$ that corresponds well to the spin-only ($S = 5/2$) effective moment of $5.91 \mu_B$ expected for high-spin Mn^{2+} . A fit of the 2D Heisenberg

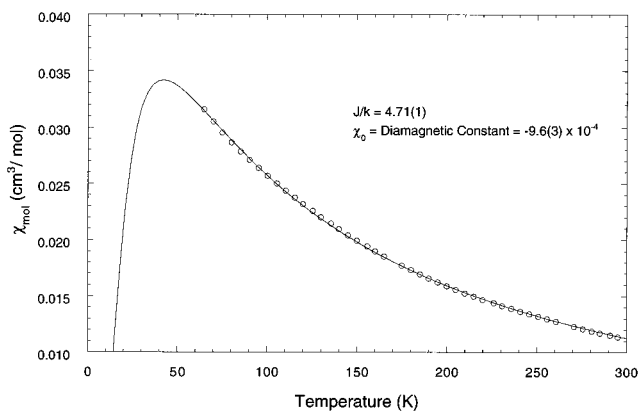


Figure 5. 2-D Heisenberg fit to the zero-field cooled (ZFC) magnetic susceptibility of $\text{Ba}_2\text{MnZn}_2\text{As}_2\text{O}_2$ (60–300 K).

model¹⁸ to the data over a temperature range of 60–300 K is shown in Figure 5 and provides the coupling constant, $J/k_B = 4.71(1)$ K. This is about half that observed for $\text{Ba}_2\text{Mn}_3\text{As}_2\text{O}_2$ (10.2(2) K).¹³ The large susceptibility and the deviation of the 2D fit below 60 K suggests that there is 3D coupling of the Mn moments in this compound. This is consistent with what is observed in $\text{Sr}_2\text{Cu}_2\text{MnO}_2\text{S}_2$, which is isostructural with alternating nonmagnetic $\text{Cu}_2\text{S}_2^{2-}$ and magnetic MnO_2^{2-} layers and shows antiferromagnetic ordering at about 30 K. However, unlike $\text{Ba}_2\text{Zn}_2\text{MnAs}_2\text{O}_2$, $\text{Sr}_2\text{Cu}_2\text{MnS}_2\text{O}_2$ shows no divergence at low temperatures of the ZFC and FC magnetization data and the 2D Heisenberg model does not fit the data.⁹ The layers are closer together in the chalcogenide compound than the pnictide compound, and it is suggested that interlayer coupling of MnO_2^{2-} gives rise to 3D magnetic ordering.⁹

The interpretation of the magnetic susceptibility of the all-Mn containing compounds has been published.¹³ The interpretation of the data was aided by a neutron diffraction study the all-Mn containing compound, $\text{Sr}_2\text{Mn}_3\text{Sb}_2\text{O}_2$.⁶ Briefly, the neutron data indicate the presence of two different magnetic lattices corresponding to the two crystallographically inequivalent Mn in these materials, one that orders near room temperature and one that orders at low temperature (50–100 K). The room-temperature magnetic lattice can be modeled as antiferromagnetic coupling both within and between the $\text{Mn}_2\text{Pn}_2^{2-}$. The low-temperature magnetic lattice can be ascribed to coupling of the MnO_2^{2-} . The low-temperature magnetic lattice is identical with that of K_2NiF_4 ,¹⁹ consisting of antiferromagnetic intraplanar interactions and ferromagnetic interactions between next nearest MnO_2^{2-} layers along c . The temperature-dependent magnetic susceptibility data for $\text{Ba}_2\text{Mn}_3\text{As}_2\text{O}_2$ is similar to $\text{Sr}_2\text{Mn}_3\text{Sb}_2\text{O}_2$ and the model of the magnetic structure can be assumed to be the same: the $\text{Mn}_2\text{As}_2^{2-}$ layer is antiferromagnetically coupled at high temperature, and the temperature-dependent magnetic susceptibility data correspond only to that of the MnO_2^{2-} layer.¹³

(16) Klüfers, P.; Mewis, A. *Z. Naturforsch. B* **1978**, *33*, 151.

(17) Pietraszko, A.; Lukaszewicz, K. *Bull. Pol. Acad. Sci. Chem.* **1976**, *24*, 459.

(18) Lines, M. E. *J. Phys. Chem. Solids* **1970**, *31*, 101.

(19) Birgeneau, R. J.; Guggenheim, H. J.; Shirane, G. *Phys. Rev. B* **1970**, *1*, 2211.

The difference between the all-Mn compound and the MnZn compound is the intervening M_2As_2 layer, and either $M = Mn$ (antiferromagnetic square lattice) or $M = Zn$ (no moment) should have no effect on the magnetic interactions within the MnO_2^{2-} plane. [The effective moment of the $Mn_2As_2^{2-}$ layer on the MnO_2^{2-} layer is expected, to first order, to be zero; there should be effectively no coupling between the pnictide and oxide layers. This is because the $Mn_2As_2^{2-}$ layer is an antiferromagnetic square lattice in which the total moment sums to zero.] Therefore, similar magnetic behavior might be expected for both $Ba_2Mn_3As_2O_2$ and $Ba_2MnZn_2As_2O_2$. However, the magnetic susceptibilities are quite different. The replacement of the intervening antiferromagnetic $Mn_2As_2^{2-}$ layer with the nonmagnetic $Zn_2As_2^{2-}$ layer results in a lower ordering temperature, an increase in the magnitude of the overall susceptibility, and differences in ZFC and FC data, and there is only weak 2D coupling in the magnetic susceptibility. The absence of a magnetically ordered intervening lattice clearly has pronounced effects on the MnO_2^{2-} magnetic interactions.

The low-temperature magnetic behavior is difficult to explain, and some speculation is provided below. Perhaps the magnetic $Mn_2As_2^{2-}$ layer in the all-Mn phase acts as an insulator between MnO_2^{2-} layers. In its absence the interlayer coupling becomes significant. If this is the case, the spin glasslike behavior may be a result of the symmetry between nearest MnO_2^{2-} layers (the layers are off-set by $1/2$, $1/2$ along x , y , providing a triangular interaction). Further studies with ac sus-

ceptibility are necessary to further probe the low-temperature magnetic state.

Summary

The $Ba_2MnZn_2As_2O_2$ compound indicates that well-ordered mixed metal phases can be obtained in the $Sr_2Mn_3As_2O_2$ structure type. The driving force for the metal segregation is the coordination preferences of Mn and Zn. The introduction of a nonmagnetic layer has a perturbation effect of the magnetic ordering of the MnO_2^{2-} layer. It results in much weaker coupling of the Mn moments within the layers with antiferromagnetic ordering at 38 K and a spin glasslike transition evident at low temperature. Further studies are underway to understand the complex magnetic behavior in this system.

Acknowledgment. We thank Enos A. Axtell, III for the sample used in neutron diffraction, Michael Price and Francisco Guerra for their contributions to the early part of this investigation, Peter Klavins for assistance, and Robert N. Shelton for the use of the SQUID magnetometer and X-ray diffractometer. We thank L. Soderholm (ANL) for useful discussion. The work is supported by NSF DMR-9505565.

Supporting Information Available: Additional single-crystal and powder X-ray diffraction and refinement data for $BaMnZn_2As_2O_2$ (4 pages). See any current masthead page for ordering and Internet access instructions.

CM970554+